Proceedings of the 2003 IEEE/RSJ
Intl. Conference on Intelligent Robots and Systems
Las Vegas, Nevada · October 2003

Time Domain Passivity Control for 6 Degrees of Freedom Haptic Displays

Carsten Preusche, Gerd Hirzinger
Institute of Robotics and Mechatronics
German Aerospace Center (DLR)
D-82234 Wessling, Germany
Carsten.Preusche@dlr.de

Jee-Hwan Ryu, Blake Hannaford
Department of Electrical Engineering
University of Washington
Seattle, WA 98195-2500, USA
jhryu@brl.ee.washington.edu

***Abstract*— In this paper a modification of the time domain passivity controller is presented to improve its performance and transparency in case of multi degrees of freedom (dof) haptic interaction. In multi-dof application the concept needs to be extended by additional conditions to distribute the adaptive damping appropriately among the degrees of freedom. This can be solved by using the geometrical information coded in the output signals of the system. Experiments show the validity of this concept.**

I. Introduction

Haptic interaction with virtual reality (VR) and in teleoperation signify an improvement for the operator working with it. Through the multimodal interaction (vision, audio and haptic) the human operator reaches a higher level of immersion and is able to explore and manipulate intuitively the virtual or remote environment [1].

There is a wide variety of applications, where haptic interaction is necessary and demanded, such as robotic assisted surgery and surgical training [2], virtual prototyping [3] and teleservice in hazard environments (e.g. space) [4].

In the fields of interaction with virtual reality and teleoperation the concept of networks and passivity is an often used method to guarantee stability of the haptic master and of the overall master-slave system ([5],[6],[7],[8],[9]). The main idea is to separate the teleoperating (virtual reality) system into different network elements, which can be made passive.

However the passivity is mostly applied in the frequency domain during the design process and is therefore conservative, because the haptic display must behave passively under all operating conditions. This means that transparency is reduced, even if not necessary. Hannaford and Ryu introduced the Time Domain Passivity Control in [10], which uses these concepts in real-time. So the amount of additional intervening dynamics (i.e. damping) can be adapted to the actual demands of the system.

This new approach will be reviewed in section II. One problem that occurs in this approach is that the damping can be introduced in different ways in the multi degree of freedom (dof) case. This paper derives one condition to distribute the necessary intervening dynamics in a transparent way for the human operator. This condition is presented in section III. In section IV the experimental results are shown, followed by some conclusions in section V.

II. Review of the Time Domain Passivity Control

In this section, a short review of the time domain passivity control is given. In figure 1 an one-port network element is shown and the positive directions of velocity and force are given to define the sign of these values. With this convention this network element is defined to be passive, if and only if ,

$$\int_0^t f(\tau)v(\tau)d\tau + E(0) \geq 0, \forall t \geq 0. \quad (1)$$

Hereby v means the velocities and f the corresponding forces. $E(0)$ is the energy initially stored in the network element at $t=0$.

This means that the initial stored energy plus the net supplied energy is always positive; a passive network element never gives more energy back to the network than it has stored at $t=0$ plus the energy received by the network.

Hannaford and Ryu introduced a so-called Passivity Observer (PO) that can measure the energy flow in real-time, assuming that the sample time is much faster than the dynamics of the system. For an one-port element the PO in the discrete domain is defined as

$$E_{obsv}(n) = \Delta T \sum_{k=0}^{n} f(k)v(k), \quad (2)$$

where ΔT is the sample time of the system. If the observed energy $E_{obsv}(n)$ is positive, the network element is passive. If the observed energy $E_{obsv}(n)$ is negative, the network element is active. The amount of energy produced by the observed network element is $-E_{obsv}(n)$. In the latter case the observed amount of "active energy" needs to be dissipated, which is done by an additional adaptive element: the so-called Passivity Controller (PC). Two different PCs were defined depending on the causality of the network element. In figure 2 the two possible PC configurations are shown.

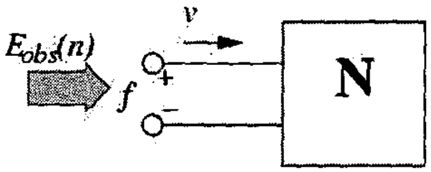

Fig. 1. Definition of velocity and force direction at an one-port network element

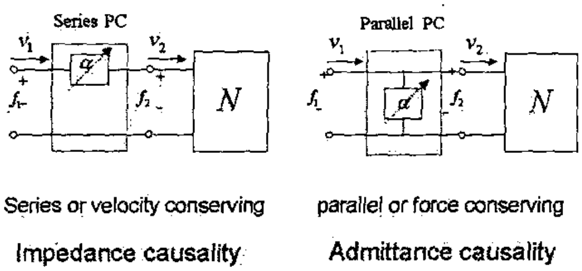

Fig. 2. Configurations of the passivity controller

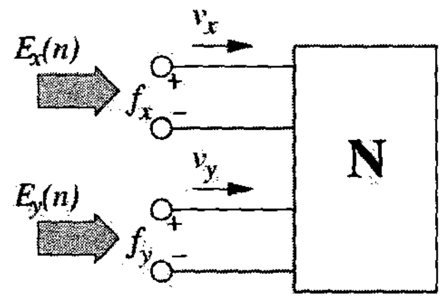

Fig. 3. Energy flow in case of a two-port element (along the main axis of the coordinate system)

For virtual environments often the impedance causality is used, where the position/velocity is read from the haptic device and the force computed by the haptic rendering algorithm. In this case the control parameter α is calculated as follows

$$\alpha(n) = \begin{cases} -\frac{E_{obsv}(n)}{\Delta T v(n)^2} & \text{if } E_{obsv}(n) < 0 \\ 0 & E_{obsv}(n) \geq 0, \end{cases} \tag{3}$$

where $E_{obsv}(n)$ is the observed energy, $v(n)$ the actual velocity and ΔT is the sampling time. The damping parameter α for the admittance causality is calculated similar based on the actual force $f(n)$.

For a more detailed description of the basic time domain passivity control see [10], [11] and [12].

Recently, two modified versions of time domain passivity controllers have been proposed to improve the performance of the PO/PC. The more accurate time domain passivity observer is proposed by removing the constant force or velocity assumption during one sampling time [13], and a reference energy following method is introduced by replacing the fixed zero energy threshold with time varying reference energy behavior to avoid exciting high frequency mode of a device [14]. These adaptations are already used in this paper.

III. Multi-DOF Extension of the PO/PC

Now the one-port is extended to a multi-port network element, e.g. the two-port element in figure 3. Then the total energy needs to be observed as a sum of all ports, like

$$\begin{aligned} E_{obs}(n) &= \sum_{k=0}^{n} f_x(k)v_x(k) \\ &\quad + \sum_{k=0}^{n} f_y(k)v_y(k) \\ &= \sum_{k=0}^{n} \mathbf{f}^T(k)\mathbf{v}(k). \end{aligned} \tag{4}$$

This can be extended easily for a n-port network element.

If the total energy is negative the network element becomes active, see example in figure 7 without the PC activation. The position of operator's tool center point contacting a virtual wall and the observed energy are shown. The energy along the Y axis is positive; the amount of energy that is generated by the contact simulation along the X axis exceeds this energy consumption and the total simulation becomes active. The PC needs to operate for dissipation of the active energy from the system. In this case many possibilities exist to apply the PC to such a system:

1) the PC can be applied only to the Y axis,
2) the PC can be applied only to the X axis (In the shown example it would increase the energy consumption of this axis to make the total energy become positive again),
3) any distribution of the PC between the two axis can be found.

The straight-forward calculation of the PO/PC will bring the following equations:

$$E_{obs}(n) = \sum_{k=0}^{n} \mathbf{f}(k)^T \mathbf{v}(k), \tag{5}$$

$$\alpha(n) = \begin{cases} -\frac{E_{obs}(n)}{\mathbf{v}(n)^T \mathbf{v}(n)} & \text{if } E_{obs}(n) < 0 \\ 0 & E_{obs}(n) \geq 0, \end{cases} \tag{6}$$

$$\mathbf{f}_{PC}(n) = \alpha(n)\mathbf{v}(n), \tag{7}$$

where α is the adaptive damping parameter within the PC for impedance causality.

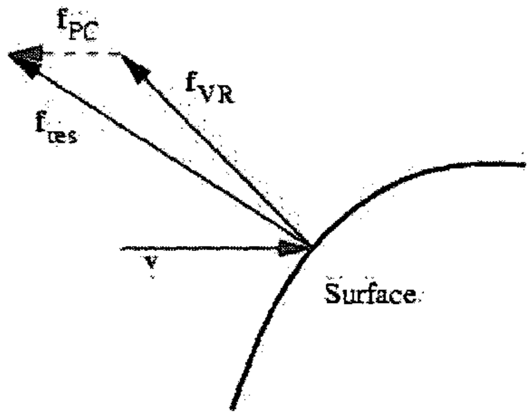

Fig. 4. Resulting forces when contacting an active surface with standard PO/PC

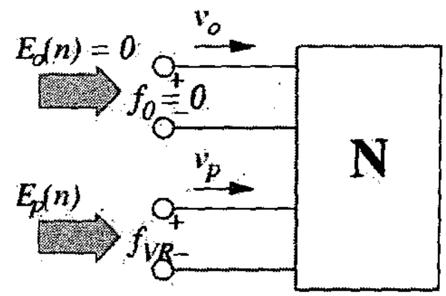

Fig. 5. Energy flow in case of a two-port element (projected to the VR force)

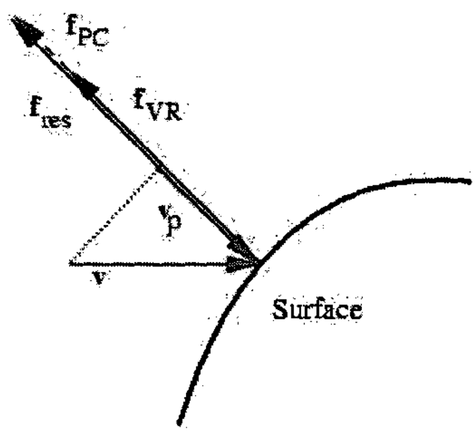

Fig. 6. Resulting forces when contacting an active surface with multi-dof PO/PC

This calculation leads to a force generated by the PC $\mathbf{f}_{PC}$ as shown in figure 4. The force vector $\mathbf{f}_{PC}$ is in the opposite direction of the master's velocity $\mathbf{v}$ and has no alignment with the force produced by the virtual environment $\mathbf{f}_{VR}$. So the direction of the resulting force $\mathbf{f}_{res}$ felt by the human operator is deflected by the operators movement. Even if the network now behaves passive this, for the operator non-causal, force disturbs the transparency of the system. For tactile exploration of objects the force direction play the most important role, because it encodes the object's shape.

If friction is not modeled in the virtual environment, the rendered force $\mathbf{f}_{VR}$ is exactly perpendicular to the object's surface. If friction is modeled, the direction of the force encodes the relation between rigidness and friction parameters of the virtual object. The additional damping from the dissipative element PC should not disturb the direction of the rendered forces, so that the impression of the shape and structure of the object is maintained.

The idea to realize this is to apply the PO/PC parallel and perpendicular to the VR output force $\mathbf{f}_{VR}$. So one port of the network element describes the energy flow associated with the virtual environment's reaction and the other port's energy flow is zero, because no force is associated with it. The direction of the resulting force is not changed and transparent for the human operator.

Actually the coordinate system of the multi-port network element is transformed such that all energy flows through only one port and the POs at the other ports have a zero energy flow (work) at this instant, see figure 5. The velocity $\mathbf{v}$ is separated into a velocity component $\mathbf{v}_p$ parallel to the force vector $\mathbf{f}_{VR}$ and a velocity component $\mathbf{v}_o$ orthogonal to it. The force $\mathbf{f}_o$ associated with $\mathbf{v}_o$ is zero and so the observed energy at this port is zero too.

The projection of the velocity $\mathbf{v}$ to the force $\mathbf{f}_{VR}$ is done by evaluating

$$\begin{aligned} \mathbf{v}_p &= \frac{\mathbf{f}_{VR}}{\|\mathbf{f}_{VR}\|} \circ \mathbf{v} \cdot \frac{\mathbf{f}_{VR}}{\|\mathbf{f}_{VR}\|} \\ &= \frac{\mathbf{f}_{VR}^T \cdot \mathbf{v}}{\|\mathbf{f}_{VR}\|^2} \cdot \mathbf{f}_{VR}. \end{aligned} \tag{8}$$

To compute the PO/PC the equations (5)-(7) are used by replacing $\mathbf{v}$ with the projected velocity $\mathbf{v}_p$. The resulting force vectors are shown in figure 6. It can be seen, that the direction of the force generated by the virtual environment is not deflected by the PO/PC. Only the length is adapted due to passivity reasons.

The calculation of the energy flow is independent of the choice of the coordinate system, as long as the coordinate system is right-angled and right-handed. The coordinate system can even be changed in each step without influence of the energy flow, if the velocity and the forces are described with in the same system at each step. With that the stability conditions and proofs for the Time Domain Passivty Controller hold also for the adaption in the multi-dof case presented here.

Using this multi-dof PO/PC the stability of the system is guaranteed and the transparency to the operator is increased. In the next section some experimental results are shown to illustrate the performance of the proposed method.

IV. Experimental Results

A 3 DoF PHANToM ([15]) connected to a simple virtual environment is used for the experiments. The PHANToM is driven by a RT-Linux system at a sampling rate of 2 kHz and the virtual environment consists of a wall with a stiffness of 5000 N/m. In the first experiments this virtual wall is planar for easier understanding of the plots and in the last experiment the virtual wall is curved to present a more general case.

First the setup is used without PC to observe the energy flow. Figure 7 shows the path of the tool center point (with the location of the virtual wall) and the observed energies for the different axes of the PHANToM. The interpretation of the figure is given in section III.

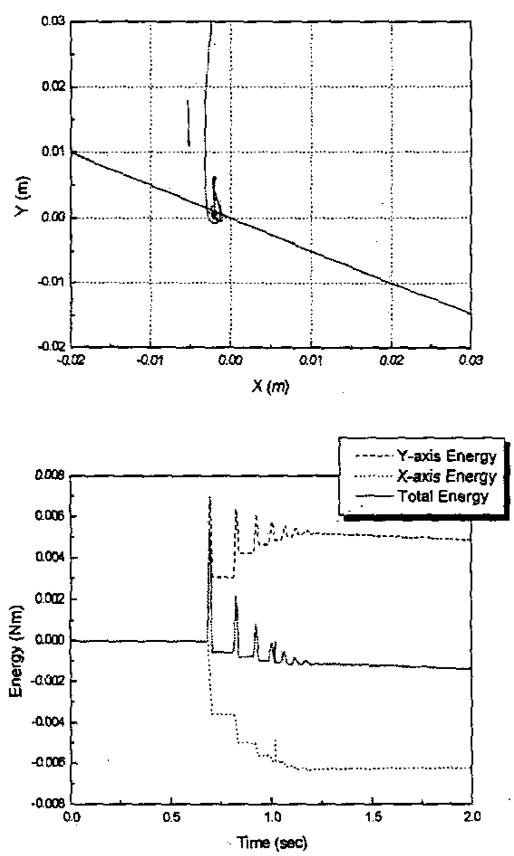

Fig. 7. Contact response without the PC for two-DOF case

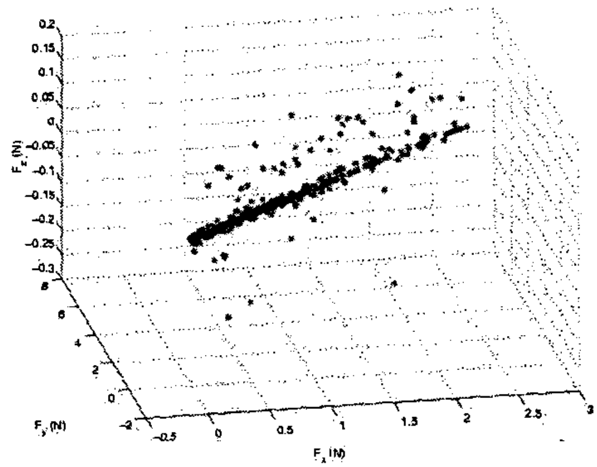

(a) without multi-dof adaptation

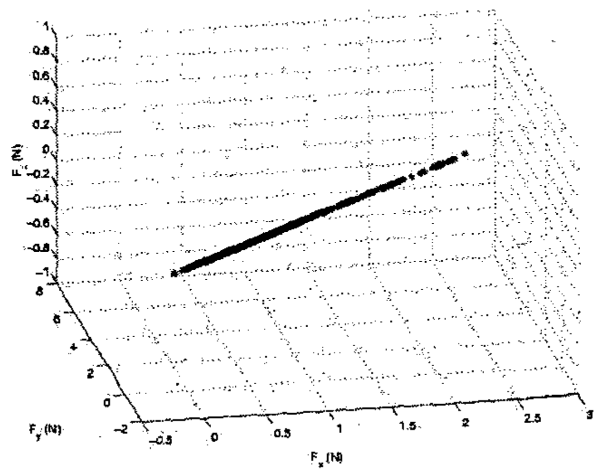

(b) with multi-dof adaptation

Fig. 8. Force vectors for a point contact experiment with the PO/PC

To compare the results of the PO/PC without and with the modification for the multi-dof case, first the force vectors for a single contact are shown. The operator is touching the virtual wall at one point and tries to keep in contact at this point. The position may vary, but the forces are expected to have the same direction (perpendicular to the wall with different sizes). In figure 8(a) the resulting force vectors without the multi-dof adaptation have mostly the same directions perpendicular to the surface of the wall, but there exist some variations. Based on the proposed control method it can be seen in figure 8(b) that the force vectors have all the same direction, but different length. So the force direction is only influenced by the virtual environment and not by the PO/PC.

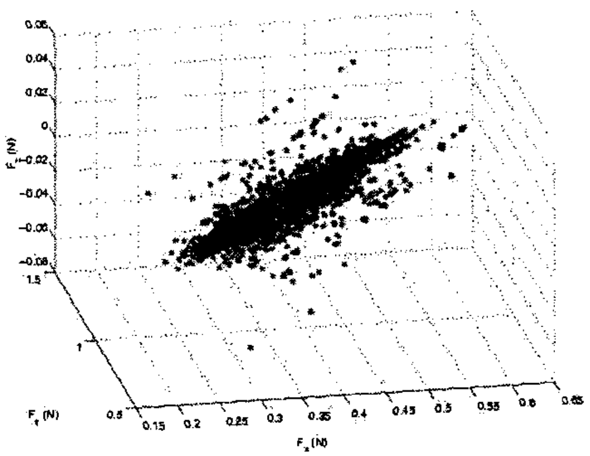

(a) without multi-dof adaptation

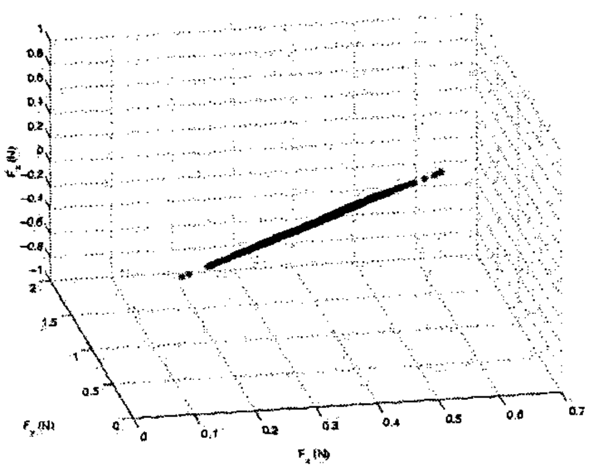

(b) with multi-dof adaptation

Fig. 9. Force vectors for a surface following experiment with the PO/PC

Now a sliding movement along the surface is made to evaluate a more dynamic interaction. Again in figure 9(a) the resulting force vectors without the multi-dof adaptation are shown. Here the amount of different force directions is big. Though one can get an impression of the main direction, signifying the surface normal, the operator feels of a very rough wall. But this gives a wrong feedback of the physical parameters of the simulated virtual wall and, which is even worse, it makes an exact movement difficult. With the multi-dof extension to the original PO/PC the direction of the force vectors only affected from the virtual environment and not from the PO/PC, see figure 9(b). So the human-felt orientation of the virtual wall is clear and smooth. This gives the operator a transparent feeling of the environment and the operator can make exact movements and manipulation in the virtual environment.

Now the operator is exploring a curved wall. In figure 10 the path of the PHANToM's tool center point is shown. The operator is touching the wall and sliding diagonal various times over the wall. The wall behaves passive, if the PO/PC is activated. The difference in the force directions using the PO/PC with and without the presented modification for multi-dof contacts are shown in figure 11. In these plots the force vector tips are projected to the tangent plane of the curved wall at the contact point. Because there is no friction modeled in the simulation, the force vector should be exactly perpendicular to the tangent plane, i.e. the force vector tip is projected to the zero point of the plane. In left plot of figure 11 the projected force vector tips of the PO/PC without modification vary around the zero point. In the right plot the force vector tips are projected exactly to the zero point of the tangent plane, i.e. all the force vectors are perpendicular to the surface of the curved wall.

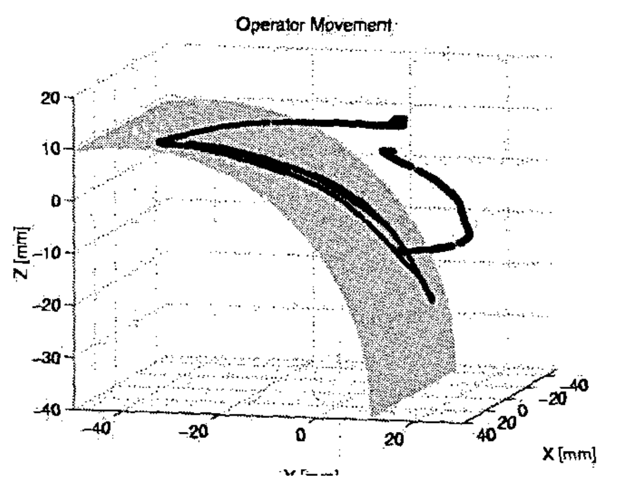

Fig. 10. Surface following at curved wall with the multi-dof PO/PC

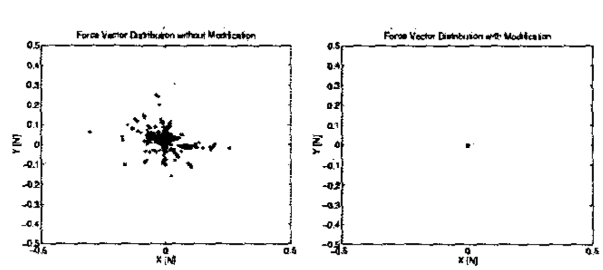

Fig. 11. Force vector tips projected to tangent plane of curved wall

In these results only three degrees of freedom are shown, but the proposed extension to the original time domain passivity control can be applied also to six degrees of freedom.

V. Conclusion and Future Works

In this paper, time domain passivity control scheme is extended for the application of the multi-dof interaction with virtual environments. With the projection of the damping force generated by the PC to the actual force direction of the virtual environment (which encodes the shape and the physical parameters of the touched object) the transparency and stability of the interaction can be improved. This approach is also valid, if additional non-linear effects like friction are rendered in the virtual environment, or if the haptic display is connected to a remote robot with force sensors.

Next this adaptation will be applied to the DLR light-weight robot as handcontroller. The multi-dof PO/PC will be used to connect the handcontroller with different haptic rendering algorithms. Acting as virtual coupling the PO/PC should stabilize any haptic rendering algorithms. The multi-dof PO/PC will be used in complex virtual environments as described in [3].

Also the combination of this approach with the introduction of the reference energy behaviour in [14] will be a research topic in the future. The reference energy will be modified, such that the constraints decribed in this paper will hold.

VI. Acknowledgments

This work was supported in part by the German Research Foundation (DFG) within the Collaborative Research Centre SFB 453 on "High-Fidelity Telepresence and Teleaction".

VII. References

[1] G. Färber and J. Hoogen, editors. *Workshop on Advances in Interactive Multimodal Telepresence Systems*, Munich, Germany, March 2001.

[2] M. C. Cavusoglu. *Telesurgery and Surgical Simulation: Design, Modeling, and Evaluation of Haptic Interfaces to Real and Virtual Surgical Environments.* PhD thesis, UC Berkeley, August 2000.

[3] C. Preusche, A. Rettig, and G. Hirzinger. Assembly Verification in Digital Mock-Ups using Force Feedback. In *12th International Symposium on Measurement and Control in Robotics Towards Advanced Robot Systems and Virtual Reality*, 2002.

[4] Klaus Landzettel, Bernhard Brunner, Alexander Beyer, Erich Krämer, Carsten Preusche, Michael Steinmetz, and Gerd Hirzinger. ROKVISS Verification of Advanced Tele-Presence Concepts for Future Space Missions. In *Proceedings of Advanced Space Technologies for Robotics and Automation*, 2002.

[5] B. Hannaford. A design framework for teleoperators with kinesthetic feedback. *IEEE Trans. on Robotics and Automation*, 5(4):426–434, August 1989.

[6] Richard J. Adams and Blake Hannaford. A two-port framework for the design of unconditionally stable haptic interfaces. In *1998 IEEE/RSJ International Conference on Intelligent Robots and Systems*, pages 1254–9. Victoria, B.C., 1998.

[7] R. J. Anderson and M. Spong. Bilateral control of operators with time delay. In *IEEE Transaction on Automatic Control*, number 34, pages 494–501, 1989.

[8] G. Niemeyer and J. Slotine. Stable adaptive teleoperation. *IEEE Journal of Oceanographic Engineering*, 16(1):152–162, 1991.

[9] T. Imaida, Y. Yokokohji, T. Doi, M. Oda, and T. Yoshikawa. Ground-Space Bilateral Teleoperation Experiment Using ETS-VII Robot Arm with Direct Kinesthetic Coupling. In *Proceedings of the IEEE International Conference on Robotics and Automation*, pages 1031–1038, Seoul, Korea, 2001.

[10] B. Hannaford and J. H. Ryu. Time Domain Passivity Control of Haptic Interfaces. *IEEE Trans. on Robotics and Automation*, 18(1):1–10, 2002.

[11] J. H. Ryu, D. S. Kwon, and B. Hannaford. Stable Teleoperation with Time Domain Passivity Control. In *Proceedings of the IEEE International Conference on Robotics and Automation*, Washington DC, USA, 2002.

[12] Jee-Hwan Ryu. *Stability Guatanteed Control for Teleoperators: Time Domain Passivity Approach.* PhD thesis, Korea Advanced Institute of Science and Technology, 2002.

[13] J. H. Ryu, Y. S. Kim, and B. Hannaford. Sampled and Continuous Time Passivity and Stability of Virtual Environments. In *Proc. of IEEE International Conference on Robotics and Automation*, Taipei, Taiwan, 2003. To be published.

[14] J. H. Ryu, B. Hannaford, C. Preusche, and G. Hirzinger. Time Domain Passivity Control with Reference Energy Behavior. In *Proc. IEEE/RSJ Int. Conf. on Intelligent Robotics and Systems*, Las Vegas, USA, Oct 2003.

[15] T.H. Massie and J.K. Salisbury. The Phantom Haptic Interface: A Device for Probing Virtual Objects. In *Proceedings of the ASME International Mechanical Engineering Congress and Exhibition*, pages 295–302, Chicago, 1994.